Recl. Trav. Chim. Pays-Bas **106**, 105–112 (1987) 0165–0513/87/04105–08$2.50

# Full papers

## Spectroscopy and reactivity of zinc 20-oxaporphyrin-IX dimethyl ester

**M. A. Hempenius, J. H. Koek and J. Lugtenburg**

*Leiden University, Org. Chem. Depart., Box 9502, 2300 RA Leiden, The Netherlands*

and

**R. Fokkens**

*Univ. of Amsterdam, Lab. Org. Chem., Nieuwe Achtergracht 129, 1018 WS Amsterdam, The Netherlands*

*(Received November 4th, 1986)*

**Abstract.** A facile method of preparing zinc 20-oxaprotoporphyrin-IX dimethyl ester (**1**) from biliverdin-IXα dimethyl ester has been found. According to NMR spectroscopy, the oxa substituent has a pronounced influence on the properties of the macrocyclic ring system. The $^1$H NMR spectrum reveals an aromatic structure and $^{13}$C NMR shows that in **1** a positive charge is delocalized, in agreement with the presence of one positive charge, and further that C-1 and C-19 have acquired the highest positive charge. This is corroborated by the reaction with nucleophiles, especially thiolates, leading to isolated adducts which could be well characterized. The adducts are the result of nucleophilic attack on the positions 1 and 19 exclusively, which agrees well with the charge on these positions in **1**. The adducts show interesting spectroscopic properties. The study of oxaporphyrins and their nucleophilic adducts may contribute to a fuller understanding of the formation and properties of bile pigments.

### Introduction

Metal porphyrins are biologically significant. Iron(II) protoporphyrin (heme) is the prosthetic group of the oxygen carriers myoglobin and hemoglobin. The active cores of catalases, peroxidases and cytochromes are formed by both iron(II) and iron(III) (Fig. 1)[1]. The iron porphyrins undergo oxidative breakdown to bile pigments; during the conversion, C-20 is lost as carbon monoxide and the iron is removed[2]. In the initial stages of the conversion, the iron-containing oxaporphyrins, verdohemochrome (Fig. 2, M = $Fe^{2+}$) and verdohemine (Fig. 2, M = $Fe^{3+}$), are involved[3].

Similarly, metal complexes of biliverdin can be cyclized to metal 20-oxaprotoporphyrin-IX derivatives[4,5]. In order to obtain information about the reactivity and the role of oxaporphyrins in living systems, we chose to examine zinc 20-oxaprotoporphyrin-IX dimethyl ester (**1**). We used zinc as coordination metal since its diamagnetic properties allow the easy use of NMR spectroscopy, while other metal ions are paramagnetic or form paramagnetic impurities. By comparing the NMR spectra of **1** with those of zinc protoporphyrin-IX dimethyl ester (ZnProto) we tried to discover how the 20-oxa substituent influences the aromaticity and charge distribution in our system. In addition, this was checked by its reactivity with various nucleophiles.

The relationship between the oxa substituent and the electronic properties of the porphyrin system is discussed. Due

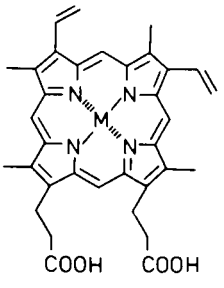


*Fig. 1. Protoporhyrin-IX (M = 2H$^+$); Heme (M = Fe$^{2+}$).*

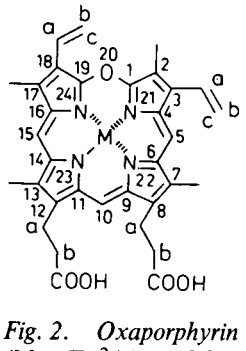


*Fig. 2. Oxaporphyrin (M = 2H$^+$), its zinc complex (M = Zn$^{2+}$), verdohemochrome (M = Fe$^{2+}$) and verdohemine (M = Fe$^{3+}$).*

to the presence of the positive charge in the system, the oxaporphyrin reacts with nucleophiles as predicted and we found evidence to show that the formation of open-chain bile pigments involves a nucleophilic attack on the oxaporphyrin system.

## Synthesis, spectroscopy and reactivity

Biliverdin-IXα dimethyl ester was prepared from bilirubin-IXα *via* published procedures[6]. According to Scheme 1, the zinc complex was obtained by reacting biliverdin-IXα dimethyl ester in THF with zinc acetate/THF solution. The colour of the reaction mixture changed from blue to bright green, the conversion being complete in one hour. Subsequently, a small excess of acetic anhydride was added and the colour changed to dull green in a few seconds. After the reaction had been quenched with water, work-up and chromatography ($SiO_2/CH_2Cl_2$) yielded **1** with the required spectral properties.

### *Mass spectrometry*

The Fast-Atom-Bombardment spectrum of **1** gave a $M^+$ signal at *m/z* 655.1826 (100%) in agreement with $C_{35}H_{35}N_4O_5Zn$ (calcd. 655.1899). The distribution of intensity of the isotopic peaks is in agreement with a 100% intensity of the $M^+$ parent molecular ion and a 17% intensity of a $(M + H)^+$ molecular ion peak (a $(M + H)^+$ signal is usually observed in (+) FAB mass spectra). The signal at *m/z* 763 (10%) originates from (M + thioglycerol)$^+$ (thioglycerol was used as a matrix compound for the optimization of the signal).

### $^1H$ *NMR*

In Fig. 3, the $^1H$ NMR spectrum of **1** (Table I) is reproduced. The H-5, H-10 and H-15 signals are visible at δ 9.08, 9.28 and 8.98 ppm. The -10 signal (δ 9.28 ppm) can be assigned by the NOE observed upon irradiation of the 8a-$CH_2$ and 12a-$CH_2$ protons (δ 3.83 ppm). Due to the overlap of 7-$CH_3$, 13-$CH_3$ and 17-$CH_3$, a similar discrimination between H-5 and H-15 cannot be made. Our assignment is based on the assumption that the H-15 signal of **1** occurs at the highest field. The order of the H-5 and H-15 chemical shifts in **1** is then the same as in ZnProto and biliverdin[8]. In Table I, the chemical shift values of the $^1H$ NMR spectra of ZnProto and **1** are presented. All signals of **1** lie at a somewhat higher field than those of ZnProto (*e.g.* 9.08, 9.28 and 8.98 ppm *versus* 10.15, 9.95 and 10.08 ppm for H-5, H-10 and H-15, resp.). This can be explained on the basis of the poorer aromatic character of **1** in which the $sp^2$ carbon on position 20 is replaced by oxygen.

It is noteworthy that of the two vinyl groups only the 18-vinyl group shows the Hc signal at a considerably lower field (6.59 ppm) than the Hc proton of the 3-vinyl group (≈6.0 ppm). This downfield shift of H-18c is not observed in the ZnProto spectrum but is present in the spectrum of biliverdin-IXα dimethyl ester. This effect, clearly induced by the 20-oxa substituent in **1**, may be caused by the through-space interaction of the proximate H-18c proton with the carbon($sp^2$)–oxygen bond (C19–O20).

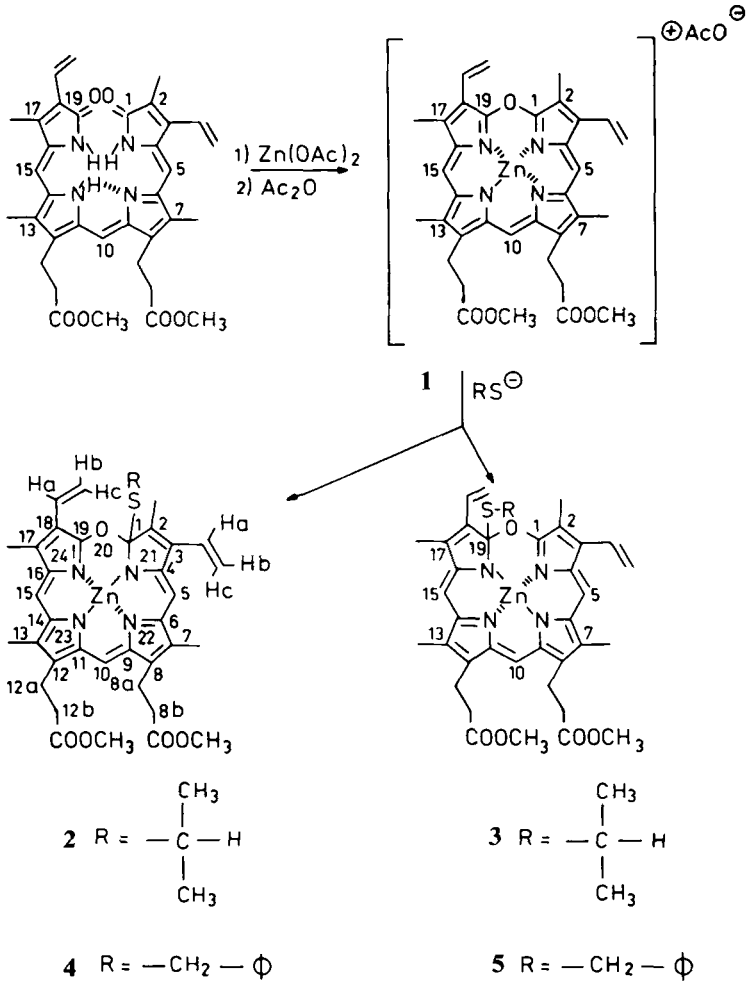


*Scheme 1. Preparation of* **1** *and its reaction with 2-propanethiolate (giving* **2** *and* **3***) and with benzylthiolate (giving* **4** *and* **5***).*

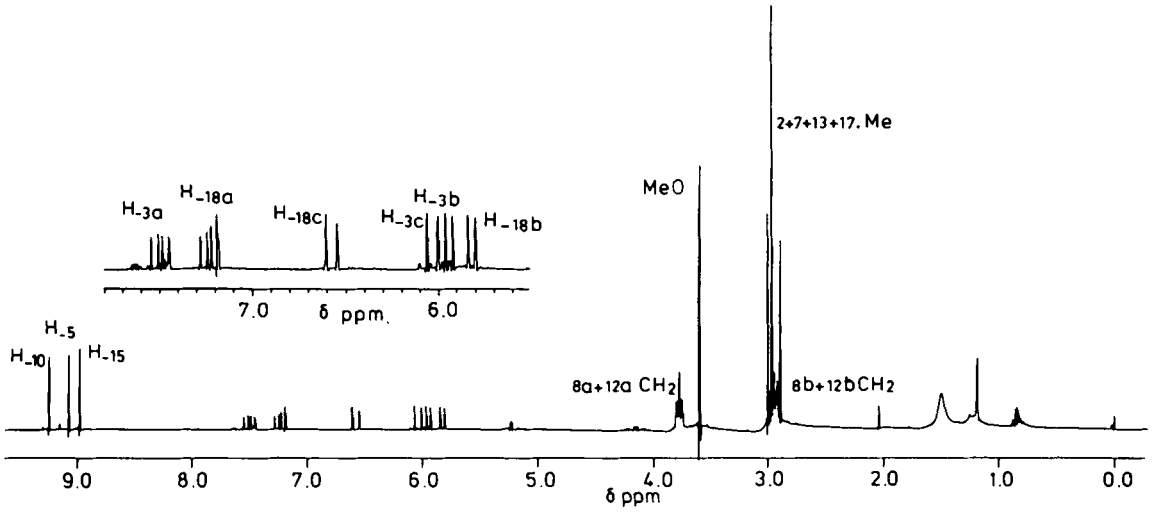


*Fig. 3. 300-MHz $^1H$ NMR spectrum of* **1** *(resolution enhanced, $CDCl_3$).*

### *$^{13}C$ NMR*

In the $^{13}C$ NMR spectrum of **1** ($CDCl_3$ + $CD_3OD$), the signals of primary, secondary, tertiary and quaternary carbons are easily identified using the APT technique, which causes the signals of primary and tertiary carbons to appear as negative and the secondary and quaternary signals to remain positive. In Fig. 4, such a $^{13}C$ NMR spectrum of **1** is reproduced. At 23.00 and 36.12 ppm, the positive signals from the secondary carbons of the a- and b-$CH_2$ groups of the propionic side-chains are recognized. The other signals in the aliphatic region (0–75 ppm) are all negative in agreement with primary signals from the methyl groups (11.33, 10.83, 10.82 and 10.63 ppm from 2-, 7-, 13- and 17-$CH_3$ and 51.80 from the methoxy groups). These signals are observed at similar positions for ZnProto (Table I)[9]. At 112.98, 113.47 and 115.34 ppm, the negative signals of the meso carbons C-5, C-10 and C-15 are seen which, for Znproto, lie at higher field (97.23, 97.52 and 98.20 ppm). The downfield shift of C-5, C-10 and C-15 is clearly caused by the effect of the positive charge which is present in the zinc oxaporphyrin system but absent in the zinc porphyrin system. The vinylic secondary carbons appear as positive signals at 119.57 and 122.70 ppm (C-18b and C-3b, respectively), while the tertiary vinylic carbons appear as negative signals at 126.14 and 127.72 ppm (C-18a and C-3a, respectively). These values are similar to those observed for the ZnProto vinylic carbons (119.04 and 131.02 ppm). In the 135–160-ppm region, small positive signals of quarternary carbons are visible. The 173.30-ppm signal is assigned to the carbonyl carbons of the propionic ester side-chains, while the signals at 161.53 and 160.69 ppm belong to C-1 and C-19. The assignment of the other quarternary signals is not clear except that most of these lie at a lower field than for ZnProto, in agreement with the delocalized positive charge in **1**. That C-1 and C-19 bear the highest positive charge is inferred from the phenomenon that the signals of carbon atoms C-1 and C-19, directly linked to the 20-oxa atom, occur at the lowest field. This is also in agreement with their reactivity towards nucleophilic attack *(vide infra)*.

### *UV/VIS spectroscopy*

In dichloromethane, dark green **1** displays two major absorptions, at $\lambda_{max}$ 680 nm (ε 14300) in the far-red and at $\lambda_{max}$ 400 nm (ε 14730), and two smaller ones at $\lambda_{max}$ 520 nm (ε 1720) and $\lambda_{max}$ 556 nm (ε 1700). The UV/VIS spectrum of ZnProto differs significantly since the 400-nm absorption

*Table I $^1H$ and $^{13}C$ NMR chemical-shift data (±0.02 ppm) of compound* **1** *and ZnProto ($CDCl_3$, ref. TMS).*

| H | 1 | ZnProto | C | 1 | ZnProto |
|---|---|---|---|---|---|
| 5 | 9.08 | 10.15 | 5 or 15 | 112.56 | 97.52 |
| 10 | 9.28 | 9.95 | 10 | 114.73 | 98.20 |
| 15 | 8.98 | 10.08 | 15 or 5 | 112.24 | 97.23 |
| 3a | 7.53 | 8.50 | 3a or 18a | 127.22 | 131.02 |
| 3b | 6.00 | 6.20 | 3b or 18b | 122.35 | 119.04 |
| 3c | 6.08 | 6.35 | | | |
| 18a | 7.25 | 8.35 | 18a or 3a | 125.56 | 131.02 |
| 18b | 5.86 | 6.10 | 18b or 3b | 119.22 | 119.04 |
| 18c | 6.59 | 6.50 | | | |
| $2CH_3$ | 2.89 | 3.76 | (2-, 7-, | (10.89 + | (12.91 + |
| $7CH_3$ | 3.02 | 3.65 | 13-, | 10.51 + | 11.77) |
| $13CH_3$ | 3.02 | 3.64 | $17CH_3$) | 10.19) | |
| $17CH_3$ | 3.02 | 3.77 | | | |
| 8a + $12aCH_2$ | 3.83 | 4.05 | 8a + $12aCH_2$ | 35.83 | 37.33 |
| 8b + $12bCH_2$ | 3.02 | 3.05 | 8b + $12bCH_2$ | 20.73 | 22.10 |
| $OCH_3$ | 3.67 | 3.67 | $OCH_3$ | 51.62 | 51.56 |

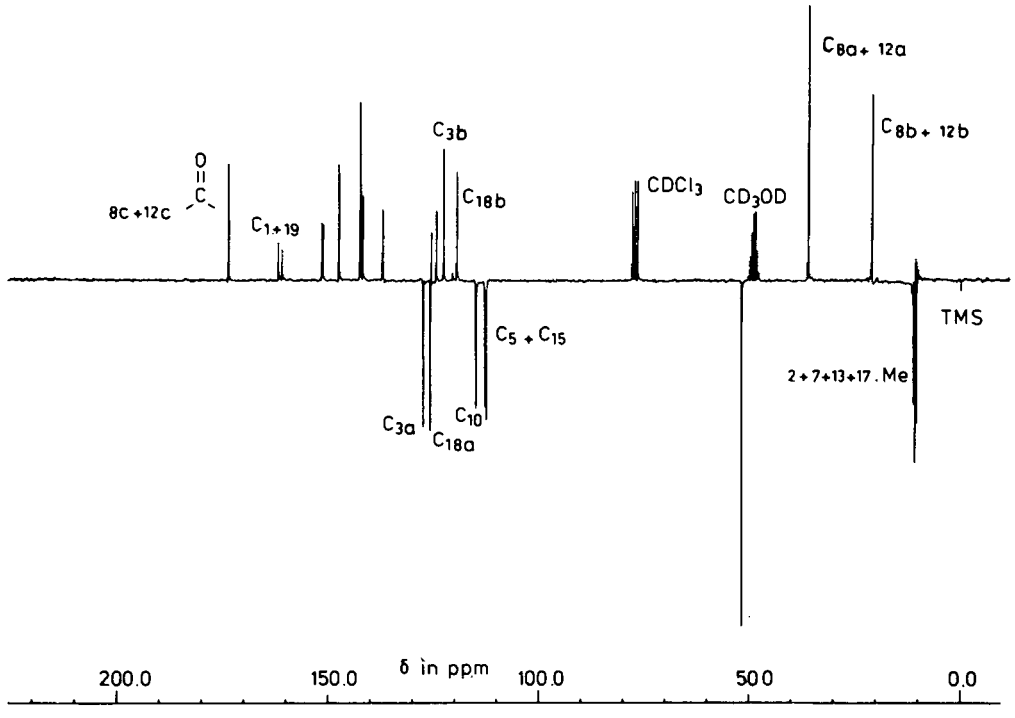


*Fig. 4. 50-MHz $^{13}C$ NMR APT spectrum of* **1** *($CDCl_3$ + $CD_3OD$).*

(Soret band) shows a much higher extinction coefficient ($\varepsilon_{max}$ 417000), two strong absorptions in the visible region ($\lambda_{max}$ 550 nm, ε 22900; $\lambda_{max}$ 589 nm, ε 24500) and no corresponding absorption in the far-red[10].

*IR spectroscopy*

The infrared spectrum of **1** shows a strong absorption from the carbonyl group of the propionic ester side-chain at 1730 $cm^{-1}$. As expected, no absorption at 1700 $cm^{-1}$ from lactam carbonyl groups (as are present in biliverdin-IXα dimethyl ester) is observed, although a strong absorption at 1220 $cm^{-1}$, caused by the asymmetric stretch of a C–O–C group in agreement with the C1–O20–C19 bond, is found. Neither biliverdin-IXα dimethyl ester nor the ZnProto system show absorptions in this region.

*Reactivity of* **1**

A solution of **1** in THF reacts with sodium 2-propanethiolate (prepared from reaction of sodium hydride with 2-propanethiol in THF). The dull green solution of **1** changes within 15 minutes into a yellow solution. Subsequently, the reaction mixture is quenched with water. Two yellow products (**2** and **3**), present in the reaction mixture (TLC), are separated by column chromatography ($SiO_2$ ether/petr. ether (40–60) 7/3). Compounds **2** and **3** are isomers of elemental composition $C_{38}H_{42}N_4O_5SZn$ (Field-Desorption mass spectrum $m/z$ = 730). Similarly, solutions of **1** with sodium benzylthiolate give the two yellow isomers **4** and **5** ($m/z$ = 778, $C_{42}H_{42}N_4O_5SZn$) which can also be isolated by preparative chromatography. In each case, two isomeric adducts are formed in which one thiolate anion has reacted with one molecule of **1**.

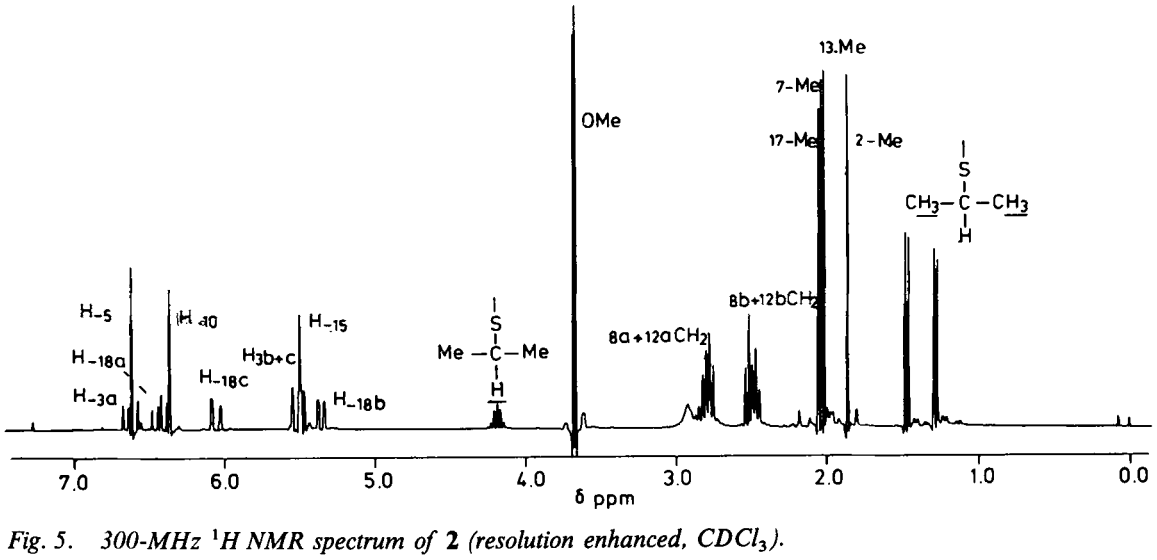


*Fig. 5. 300-MHz $^1H$ NMR spectrum of* **2** *(resolution enhanced, $CDCl_3$).*

According to TLC analysis, reaction of **1** with KCN (crown ether) or with sodium borohydride also gives two yellow products in both cases. However, these species are too unstable to be either isolated or characterized. Field--Desorption mass spectra of **1** from targets loaded with methanol display a peak at *m/z* 686 ($C_{36}H_{38}N_4O_6Zn$) corresponding to nucleophilic addition of methanol to **1**.

*Spectroscopic properties of the thiolate adducts*

In the infrared spectra of **2**, **3**, **4** or **5**, no other carbonyl signals, besides those due to the propionic ester side-chain (1730 $cm^{-1}$), are observed. As in the case of **1**, there is, at 1215 $cm^{-1}$, a strong absorption from an asymmetric C–O–C stretch, demonstrating an intact C1–O20–C19 bond. It is clear that no ring opening to biliverdin-type systems has occurred (*c.f.* the strong IR absorption at 1700 $cm^{-1}$ and the lack of significant absorption in the 1215-$cm^{-1}$ region of biliverdin-IXα dimethyl ester).

In Fig. 5, the 300-MHz $^1$H NMR spectrum of **2** is reproduced, which in many ways resembles that of **1**. The signals are only shifted somewhat upfield and extra signals, from the presence of the 2-propanethiolate group, are visible. This implies, as is expected from a thiolate adduct of **1**, that the overall structure of **2** is similar to that of **1**.

The assignment of the 2-, 7-, 13- and 17-$CH_3$ and the H-5, H-10 and H-15 signals could be effected by NOE studies. Irradiation of the signal of H-8a + H-12a (2.83 ppm) gives a NOE on the singlet at 6.41 ppm. This signal thus belongs to H-10. Irradiation of the signal at 1.86 ppm, not giving a NOE at the low field singlets, shows that this signal belongs to the 2-methyl group. Only irradiation of the 2.05-ppm signal enhances the 6.66-ppm singlet, establishing that the signals belong to the 7-methyl and H-5, respectively. Each of the two remaining signals δ 1.99 and 2.03 ppm (13- and 17-methyl) gives a NOE on the singlet at 5.50 ppm in agreement with the expected assignment.

Using double-resonance techniques, the remaining signals at low field were assigned to two different vinyl groups (at C-3 and C-10). Irradiation of the 17-methyl signal (2.03 ppm) enhances the Ha (H-18a) signal of one of the vinyl groups making the low field assignment complete.

The signals of the 2-propanethiolate group are clear, *i.e.* doublets at 1.18 and 1.48 ppm for the methyls (*J* 6.7 Hz) and, at 4.17 ppm, the heptet due to the methine proton (*J* 6.7 Hz). The two diastereotopic methyl groups show a considerable chemical-shift difference, while the two ester methyls, which can be observed at 3.69 ppm, differ only slightly in chemical shift.

Thus, **2** and **3** are isomers which differ in the place of attachment of the thiolate group to the porphyrin ring. In view of the close similarity of the $^1$H NMR parameters of the skeleton protons, the place of attachment is either 1 or 19, *i.e.* **2** and **3** are structural isomers; one has the thiolate group attached at position 1 and the other at 19 or the reverse.

In the $^1$H NMR spectrum of **2**, the signal of H-18c is observed in the same region as for **1** and for biliverdin-IXα dimethyl ester. Hence, in **2**, C-19 has $sp^2$ hybridization just as in **1** and in biliverdin-IXα dimethyl ester. This can only be the case when in **2** the thiolate group is attached at C-1. This also indicates that in **3** the place of attachment is C-19 and in the $^1$H NMR spectrum of **3** the H-18c does indeed show a regular chemical shift value as do the protons in the other vinyl group (H-3b, H-3c; Fig. 6).

There is also a resemblance between the $^1$H NMR spectra of **4** and **2** on the one hand and of **5** and **3** on the other (Fig. 6), indicating that, in the isomeric pair **4** and **5**, the thiolate group is attached to C-1 in **4** and to C-19 in **5**. This

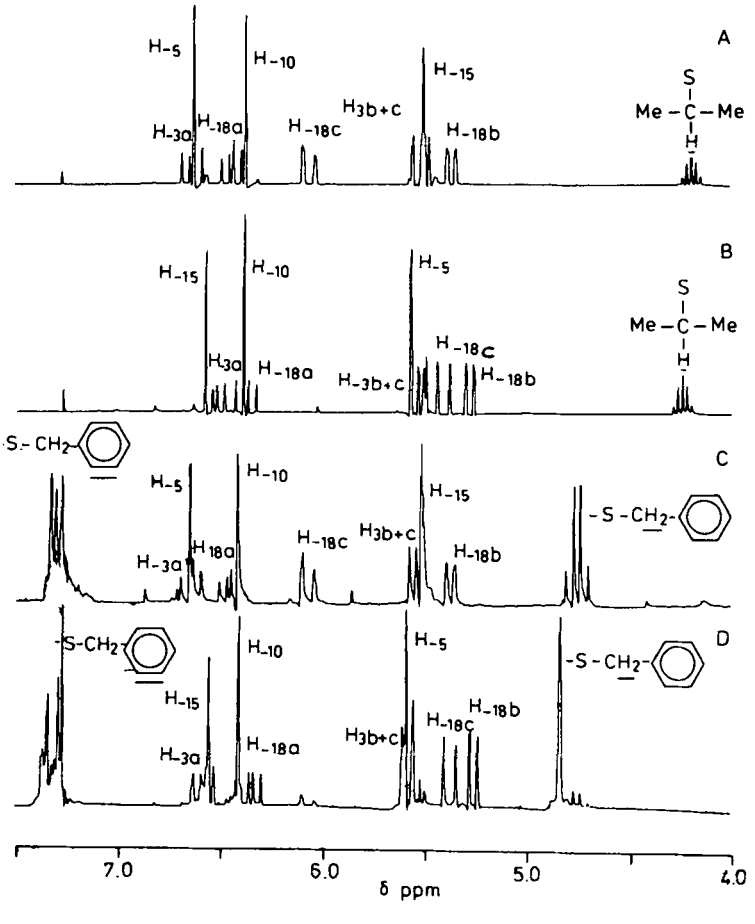


*Fig. 6. The 7.5–4.0 regions of the 300-MHz $^1$H NMR spectra of* **2**, **3**, **4** *and* **5** *(resolution enhanced, $CDCl_3$).*

also appears from the chemical-shift parameters of H-18c having the special low chemical-shift value in **4** and a higher value in **5** (Table II).

*Table II* $^1H$ *NMR chemical-shift data (±0.02 ppm) of the thiolate adducts*[a].

| H | 2 | 4 | 3 | 5 |
|---|---|---|---|---|
| 5 | 6.66 | 6.63 | 5.56 | 5.57 |
| 10 | 6.41 | 6.40 | 6.39 | 6.39 |
| 15 | 5.50 | 5.50 | 6.58 | 6.54 |
| 3a | 6.64 | 6.63 | 6.52 | 6.55 |
| 3b | 5.49 | 5.49 | 5.50 | 5.55 |
| 3c | 5.50 | 5.52 | 5.52 | 5.56 |
| 18a | 6.44 | 6.44 | 6.36 | 6.33 |
| 18b | 5.36 | 5.35 | 5.28 | 5.24 |
| 18c | 6.05 | 6.04 | 5.40 | 5.36 |
| 2-$CH_3$ | 1.86 | 1.86 | 1.84 | 1.85 |
| 7-$CH_3$ | 2.05 | 2.08 | 2.00 | 1.94 |
| 13-$CH_3$ | 1.99 | 1.99 | 2.09 | 2.06 |
| 17-$CH_3$ | 2.03 | 2.05 | 2.20 | 2.16 |
| 8a- + 12a-$CH_2$ | 2.83 | 2.80 | 2.82 | 2.82 |
| 8b- + 12b-$CH_2$ | 2.52 | 2.50 | 2.50 | 2.50 |
| $OCH_3$ | 3.69 | 3.67 | 3.67 | 3.65 |
| SCH< | 4.17 | – | 4.23 | – |
| $SCH(CH_3)_2$ | 1.48 + 1.18 | – | 1.50 + 1.30 | – |
| Aryl-H | – | 7.29 | – | 7.32 |
| $SCH_2Ar$ | – | 4.77 + 4.72 | – | 4.82 |

[a] **2,4** and **3,5** are grouped together for easy comparison of their similar structure ($CDCl_3$, ref. TMS).

In the $^{13}C$ NMR spectra of **2** and **3**, the signals for the primary, secondary and tertiary carbons are readily assigned, corroborating the proposed structures of **2** and **3** as depicted in Scheme I. The amounts of **4** and **5** were too small to obtain $^{13}C$ NMR spectra with sufficient signal intensity. For compounds **2** and **3**, the low-field signals at 173.3 and 173.0 ppm are assigned to the carbonyls of the propionic ester side-chain at positions 8 and 12. Fifteen small peaks in the region of 170 to 130 ppm correspond to the quarternary $sp^2$ carbons, however their assignment to individual carbon atoms cannot be made. It also proved impossible to detect the quaternary $sp^3$ carbon signal of C-1 for **2** or C-19 for **3** (to which the thiolate group is attached). This may be due to low intensity related to the long relaxation time. Addition of the relaxation agent manganese acetylacetonate ($Mn(acac)_3$), which lowers the relaxation time in many cases[11], leads only to deterioration of all the $^{13}C$ signals, presumably due to reaction of the $Mn(acac)_3$ with **2** and **3**.

*Table III UV/VIS data (nm) of thiolate adducts* **2**, **3**, **4** *and* **5** *(solv.* $CH_2Cl_2$*).*

| Comp. | $\lambda_{max}$ (ε) |
|---|---|
| **2** | 430 (8250), 880 (2700) |
| **3** | 450 (8000), 860 (3020) |
| **4** | 430 (7600), 880 (2380) |
| **5** | 450 (7250), 860 (2680) |

*UV/VIS spectroscopy*

In Table III, the $\lambda_{max}$ and $\varepsilon_{max}$ values of **2**, **3**, **4** and **5** are presented. It is clear that the $\lambda_{max}$ values of **2** and **4** are virtually identical, just as in the case of the other pair (**3** and **5**). The $\varepsilon_{max}$ values show a similar trend. This is in agreement with the fact that **2** and **4** have the thiolate substituent attached to the same carbon atom (C-1) and thus have an identically conjugated system which differs from that of **3** and **5** (attachment to C-19). The UV/VIS spectrum of the thiolate adduct **2** displays, in addition to an intense absorption at $\lambda_{max}$ 430 nm (ε 8250), a weak absorption in the near-infrared region at $\lambda_{max}$ 880 nm (ε 2700). Zinc oxaporphyrin and zinc porphyrin do not show any absorptions at such long wavelengths whereas the thiolate adduct does. Their extinction coefficients are much higher and the long-wavelength $\lambda_{max}$ values are more hypsochromic. It is clear that the addition of the thiol induces a drastic change in the electronic system of the oxaporphyrin and that the absorption in the near infrared is indicative of the long-conjugated electronic system.

## Discussion

An efficient and mild preparation of zinc 20-oxaporphyrin-IX dimethyl ester (**1**) from biliverdin-IXα dimethyl ester has been found. The preparation of the latter from bilirubin-IXα *via* mild methods is also described. The spectroscopic properties of **1** are in agreement with the previously described zinc oxaporphyrins[4,5], although more detailed information is now available from its 300-MHz $^1H$ NMR and $^{13}C$ NMR spectra. The aromaticity of **1** is somewhat less than that of the corresponding ZnProto, as is deduced from the upfield-shifted chemical-shift values of H-5, H-10 and H-15 compared with those of ZnProto. Evidently, the ring current is perturbed by the 20-oxa substituent. This result is in agreement with the reported X-ray structure of **1**[12].

The signals in the $^{13}C$ NMR spectrum are less sensitive to ring current effects and more sensitive to the effects of electric charge than those in the $^1H$ NMR spectrum. These $^{13}C$ signals are observed at lower field than those of Znproto which is in agreement with the presence of one positive charge in **1**. This indicates that, in **1**, this positive charge is strongly delocalized. The signals of C-1 and C-19 occur at the lowest field which may indicate that these positions have the highest density of positive charge, even bearing in mind that the oxa substituent may also have an effect on the chemical shift.

ZnProto is generally inert upon reaction with nucleophiles (*e.g.* thiolates) as indeed are all neutral metal porphyrins[13]. Compound **1**, however, readily reacts with various nucleophiles with complete conversion to form neutral addition products. In the case of 2-propane- and benzyl-thiolate, these products can be isolated. In both cases, two isomeric thiolate adducts are formed with an intact macro oxa-ring structure (**2**, **3**, **4** and **5**). These adducts differ in the attachment of the thio substituent. In **2** and **4**, the attachment is at C-1 and in **3** and **5** at C-19. No other products are formed. This is in agreement with the fact that, according to the $^{13}C$ NMR spectrum, the amount of positive charge is highest at positions 1 and 19 in **1**. Infrared spectroscopy in particular strongly favours cyclic structures for **2**, **3**, **4** and **5** over possible ring-opened structures.

Other nucleophiles, such as cyanide and sodium borohydride, give complete reactions with **1**, although these products are too unstable for full characterization. However, their UV/VIS spectra show a close resemblance to those of **2**, **3**, **4** and **5**, leading us to assume that, in these other cases, attack also takes place at the positions 1 and 19 in **1**. The reaction of **1** with hydroxide and methanolate in solution does not lead to clear results, however, in the field desorption mass spectra of **1** from targets loaded with methanol, a peak corresponding to nucleophilic attack of methanolate on **1** is found, similar to the thiolate adducts.

Both the easy formation of oxaporphyrin from biliverdin and the facile nucleophilic reactions of nucleophiles at C-1 and C-19 in **1** indicate that oxaporphyrins are likely precursors in biliverdin formation and that their adducts

are important for a full understanding of the chemistry of bile pigments.

## Experimental

The bilirubin-IXα, dichlorodicyanoquinone (DDQ), 2-propanethiol and benzylthiol were purchased from Janssen and the zinc acetate from Aldrich. The THF was dried over $LiAlH_4$ and freshly distilled prior to use. Ether, petroleum ether (40–60°C fraction) and dichloromethane were dried over $P_2O_5$ and were also distilled prior to use. The $^1H$ NMR spectra were measured using a Bruker WM 300 spectrometer with TMS as internal standard. The $^{13}C$ NMR spectra were recorded on a JEOL FX 200 spectrometer also with TMS as internal standard. The infrared spectra were determined on a Beckman IR spectrophotometer and the UV/VIS spectra on a Cary 219 spectrophotometer. The Field-Desorption (FD) mass spectra were obtained using a Varian MAT 711 mass spectrometer with a combined EI/FI/FD source. The samples were dissolved in chloroform and an emitter current of 15–20 mA was used to desorb the samples. The spectra were obtained using an ultraviolet chart recorder. The Fast-Atom-Bombardment (FAB) mass spectrometry was carried out using a VG Analytical ZAB-HF mass spectrometer, an instrument with reversed geometry and fitted with a high field magnet and coupled to a V.G. 11-250 data system. The samples were loaded in 1-thioglycerol onto a stainless steel probe and bombarded with xenon atoms having 8 KeV energy. During the high-resolution FAB-MS measurements, a resolving power of 25000 (10% valley definition) was used.

*Biliverdin-IXα dimethyl ester*

By adding dropwise, with gentle swirling, an ethereal solution of diazomethane (prepared from nitrosomethylureum and alkaline) to a suspension of 250 mg of bilirubin-IXα in 250 ml of dichloromethane, a clear solution of bilirubin dimethyl ester was prepared. After complete conversion (TLC: alumina 2% $MeOH/CH_2Cl_2$), one drop of acetic acid was added to remove unreacted diazomethane and the solution was concentrated to 50 ml. A solution of 120 mg of dichlorodicyanoquinone (DDQ) in 100 ml of $CH_2Cl_2$ was then added and the yellow colour turned to dark blue. After the reaction was complete (TLC: alumina 2% $MeOH/CH_2Cl_2$), the reaction mixture was washed once with a sodium bicarbonate/sodium chloride solution and twice with saturated sodium chloride solution. The organic layer was dried over anhydrous sodium sulfate, filtered and evaporated. The residue was chromatographed over alumina, using 2% $MeOH/CH_2Cl_2$ as eluent to yield 212 mg of a dark solid (81%), the spectroscopic data of which were identical to those previously reported.

*Zinc oxaporphyrin dimethyl ester complex*

A solution of 0.8 g of zinc acetate in 150 ml of THF (dissolved by gently heating) was added to 0.2 g of biliverdin dimethyl ester in 50 ml of THF and the mixture stirred for $\frac{1}{2}$ h. The colour changed from blue to bright green showing the formation of the zinc complex. A solution of 0.3 g of acetic anhydride in 50 ml of THF was then added in one portion to the reaction mixture with vigorous stirring. After eight seconds, the reaction mixture was quenched by pouring it into a separating funnel containing 100 ml of dichloromethane and 250 ml of an aqueous solution of sodium bicarbonate and sodium chloride, immediately upon which the mixture was thoroughly shaken. The layers were separated and the dark green organic phase twice washed with water containing sodium chloride, dried over anhydrous sodium sulfate, filtered and evaporated. The residue was chromatographed over silica, using 10% acetone/dichloromethane as eluent, to yield 163 mg (68%) of a dull green solid. FAB-MS mass calcd. for $C_{35}H_{35}N_4O_5Zn$ ($M^+$): 655.1899, found 655.1826. Obs. fragm.: 655 (100%), 656 (59%), 657 (78%), 658 (47%), 659 (54%), 660 (25%); calcd. fragm. for 100% $M^+$ and 17% $(M+H)^+$: 655 (100%), 656 (59%), 657 (74%), 658 (45%), 659 (54%), 660 (26%). IR (KBr): 1730 $cm^{-1}$ (C=O), 1220 $cm^{-1}$ (C1–O20–C19), 1170 $cm^{-1}$ (C–O, ester). UV/VIS ($CH_2Cl_2$): $\lambda_{max}$ 400 nm (ε 14730), 520 nm (ε 1720), 556 nm (ε 1700), 680 nm (ε 14300). The $^1H$ NMR data are presented in Table I. $^{13}C$ NMR ($CDCl_3$): 173.39 (C=O), 161.53 + 160.69 (C-1 + C-19), 151.23 + 150.93 + 147.17 + 142.26 + 142.12 + 142.0 + 141.53 + 136.87 + 136.74 + 125.0 + 124.2 (C-2 + C-3 + C-4 + C-6 + C-7 + C-8 + C-9 + C-11 + C-12 + C-13 + C-14 + C-16 + C-17 + C-18), 127.22 + 125.56 (C-3a + C-18a), 122.35 + 119.22 (C-3b + C-18b), 114.73 (C-10), 112.56 + 112.24 (C-5 + C-15), 51.62 (8- + 12-$OCH_3$), 35.83 (C-8a + C-12a), 20.73 (C-8b + C-12b), 10.89 + 10.51 + 10.19 (2- + 7- + 13- + 17-$CH_3$).

*Reaction of 2-propanethiolate with* **1**

The thiolate anion was prepared by adding 0.2 ml of 2-propanethiol to a stirred suspension of 25 mg of sodium hydride (prepared from 50 mg of sodium hydride 50% suspension) in 25 ml of THF under a nitrogen atmosphere. After 1 h of stirring at room temperature, the thiolate was added portionwise (0.5 ml) to a solution of 50 mg of **1** in 80 ml of THF. About 8.5 ml of the thiolate solution is required for the conversion (TLC: silica 4% $MeOH/CH_2Cl_2$). The reaction mixture was poured into water/dichloromethane and the organic layer separated, twice washed with an aqueous saturated sodium chloride solution, dried over sodium sulfate, filtered and evaporated. The residue was chromatographed over silica, using ether/petr. ether 7/3 as eluent, to yield two yellow fractions, first 13 mg of **2** and then 12 mg of **3**.

Spectroscopic data of **2**. FD-nominal Mass *m/z* 730 ($C_{38}H_{42}N_4O_5SZn$). UV/VIS ($CH_2Cl_2$): $\lambda_{max}$ 430 nm (ε 8250), 880 nm (ε 2700). IR (KBr): 1730 $cm^{-1}$ (C=O), 1220 $cm^{-1}$ (C1–O20–C19), 1170 $cm^{-1}$ (C–O, ester). The $^1H$ NMR data are presented in Table II. $^{13}C$ NMR ($CDCl_3$): δ 173.27 + 172.95 (C=O), 170.70 (C-19), 164.3, 157.30, 149.20, 147.96, 147.02, 146.22, 142.35, 141.27, 140.39, 134.93, 132.16, 131.75, 130.44, 128.10 (C-2 + -3 + -4 + -6 + -7 + -8 + -9 + -11 + -12 + -13 + -14 + -16 + -17 + -18), 127.60 (C-3a), 126.73 (C-18a), 120.27 (C-3b), 119.98 (C-18b), 118.73 (C-5), 114.84 (C-10), 94.11 (C-15), 51.62 + 51.54 (8- + 12-$OCH_3$), 38.19 (SCH⟨), 35.19 + 34.95 (C-8a + -12a), 19.77 (C-8b + -12b), 23.97 + 22.60 ($SCH(CH_3)_2$), 10.66 (7-$CH_3$), 9.58 (17-$CH_3$), 9.37 (13-$CH_3$), 9.17 (2-$CH_3$).

Spectroscopic data of **3**. FD-nominal Mass *m/z* 730 ($C_{38}H_{42}N_4O_5SZn$). UV/VIS ($CH_2Cl_2$): $\lambda_{max}$ 450 nm (ε 8000), 860 nm (ε 3020). IR (KBr): 1740 $cm^{-1}$ (C=O), 1220 $cm^{-1}$ (C1–O20–C19), 1170 $cm^{-1}$ (C–O, ester). The $^1H$ NMR data are presented in Table II. $^{13}C$ NMR ($CDCl_3$): δ 173.33 + 173.04 (C=O), 170.27 (C-1), 164.81, 156.83, 149.24, 148.04, 146.53, 146.12, 142.61, 140.86, 140.66, 135.11, 132.19, 131.90, 130.64 (C-2 + -3 + -4 + -6 + -7 + -8 + -9 + -11 + -12 + -13 + -14 + -16 + -17 + -18), 127.19 (C-3a + C-18a), 120.45 (C-3b), 117.27 (C-18b), 118.11 (C-15), 114.81 (C-10), 94.14 (C-5), 51.74 + 51.65 (8- + 12-$OCH_3$), 38.40 (SCH⟨), 35.33 + 34.98 (C-8a + -12a), 19.71 (C-8b + -12b), 23.86 + 22.63 ($SCH(CH_3)_2$), 10.83 (17-$CH_3$), 10.07 (13-$CH_3$), 9.46 (7-$CH_3$), 9.31 (2-$CH_3$).

*Reaction of benzylthiolate with* **1**

The reaction was carried out as described above with the exception that only 20 mg of sodium hydride was required (from 40 mg of the suspension). A more rapid reaction is observed. Yield 12 mg of **4** and 3 mg of **5** after chromatography.

Spectroscopic data of **4**. FD-nominal Mass *m/z* 778 ($C_{42}H_{42}N_4O_5SZn$). UV/VIS ($CH_2Cl_2$): $\lambda_{max}$ 430 nm (ε 7600), 880 nm (ε 2380). IR (KBr): 1730 $cm^{-1}$ (C=O), 1220 $cm^{-1}$ (C1–O20–C19), 1170 $cm^{-1}$ (C–O, ester). The $^1H$ NMR data are presented in Table II.

Spectroscopic data of **5**. FD-nominal Mass *m/z* 778 ($C_{42}H_{42}N_4O_5SZn$). UV/VIS ($CH_2Cl_2$): $\lambda_{max}$ 450 nm (ε 7250), 860 nm (ε 2680). IR (KBr): 1740 $cm^{-1}$ (C=O), 1220 $cm^{-1}$ (C1–O20–C19), 1170 $cm^{-1}$ (C–O, ester). The $^1H$ NMR data are presented in Table II.

## Acknowledgements

The authors wish to thank Prof. dr. *J. C. Lagarias* for valuable discussions as to the role of oxaporphyrins in the heme catabolism and Prof. dr. *N. M. M. Nibbering* (University of Amsterdam) for his valuable suggestions. Drs. *C. Erkelens* recorded the 300 MHz $^1H$ NMR spectra and Mr. *F. Lefeber*

measured the $^{13}C$ NMR spectra. We also wish to thank Mrs. *S. Amadio* and Mrs. *K. v.d. Hoef* for reading the manuscript critically. *R. Fokkens* would like to thank the Netherlands Organization for Pure Research (SON/ZWO) for the grant to purchase the V.G. ZAB-HF mass spectrometer.

## References

[1] *J. W. Buchler*, "The Porphyrins", part I, ed. *D. Dolphin*, Acad. Press, N.Y., 1979, p. 447.
[2] *R. Schmid* and *A. F. McDonagh*, "The Porphyrins", part VI, ed. *D. Dolphin*, Acad. Press, N.Y., 1979, p. 257.
[3] *S. Saito* and *H. A. Itano*, Proc. Natl. Acad. Sci. USA **79**, 1393 (1982).
[4] *J. H. Fuhrhop, A. Salek, J. Subramanian, C. Mengersen* and *S. Besecke*, Lieb. Ann. Chem. 1131 (1975).
[5] *S. Saito* and *H. Itano*, J. Chem. Soc. Perkin Trans. I 1 (1986).
[6] *H. Fischer, H. Plieninger* and *O. Weissbarth*, Hoppe Seylers Z. Physiol. Chem. **268**, 197 (1941) and *H. Plieninger, F. El-Barkawii, K. Ehl, R. Kohler* and *A. F. McDonagh*, Ann. Chem. **758**, 195 (1972).
[7] *R. J. Abraham, F. Eivazi, R. Nayyir-Mazhir, H. Pearson* and *K. M. Smith*, Org. Magn. Res. **11**, 652 (1978).
[8] *H. Lehner, S. E. Braslavsky* and *K. Schaffner*, Lieb. Ann. Chem. 1990 (1978).
[9] *R. J. Abraham, S. C. M. Fell* and *H. Pearson*, J. Chem. Soc. Chem. Com. 699 (1976).
[10] *J. W. Buchler*, "The Porphyrins", part I, ed. *D. Dolphin*, Acad. Press, N.Y., 1979, p. 414 and *H. Fischer* and *B. Püher*, Hoppe Seylers Z. Physiol. Chem. **154**, 59 (1926).
[11] *A. M. v.d. Braken-van Leersum, C. Tintel, M. van 't Zelfde, J. Cornelisse* and *J. Lugtenburg*, to be published in Recl. Trav. Chim. Pays-Bas.
[12] *J. H. Fuhrhop, P. Krüger* and *W. S. Sheldrick*, Lieb. Ann. Chem. 339 (1977).
[13] *J. H. Fuhrhop*, "The Porphyrins", part II, ed. *D. Dolphin*, 1979, Acad. Press, New York, p. 131.

Recl. Trav. Chim. Pays-Bas **106**, 112–119 (1987) 0165–0513/87/04112–07$2.25

# Bacteriorhodopsin. The influence of the cyclohexene-ring methyls

**J. M. L. Courtin, L. Verhagen, P. L. Biesheuvel and J. Lugtenburg**

*Department of Organic Chemistry, Leiden University, 2300 RA Leiden, The Netherlands*

and

**R. L. van der Bend and K. van Dam**

*Department of Chemistry, B.C.P. Janssen Instituut, University of Amsterdam, 1018 TV Amsterdam, The Netherlands*
*(Received November 26th, 1987)*

**Abstract.** Four ring-demethylated retinals, *viz.* 1,1′,5-tridemethylretinal,1,1′-didemethylretinal, 1,5--didemethylretinal and 1-didemethylretinal, have been synthesized via new and simple schemes. The properties of these modified retinals, their protonated *Schiff* bases and the corresponding bacteriorhodopsins have been studied and compared with the native system. These bacteriorhodopsin analogues have also been tested for their proton-pump efficiencies. A large decrease in proton-pump activity was found for the analogues lacking the 5-methyl group. On the whole, the opsin shifts of the modified bacteriorhodopsins were much lower than those of the native system. UV-Vis and $^1H$ NMR data support a planar 6-*s*-*trans* conformation for the demethylated retinals in solution rather than a twisted 6-*s*-*cis* conformation (torsion angle 40–60°) as found in retinal. This explains the lower opsin shift and the better fit of these demethylated retinals in bacteriorhodopsin's binding site, which, in its native form, contains a 6-*s*-*trans* chromophore.

## 1 Introduction

Chromo-proteins with a retinylidene chromophore such as bacteriorhodopsin, as well as visual pigments and retinochrome, are important in photobiology[1]. Bacteriorhodopsin (hereafter referred to as bR), the light-energy-converting protein of the purple membrane of the halophilic micro-organism *Halobacterium halobium*,occurs in a light--adapted ($bR^{LA}_{568}$; $\lambda_{max}$ 568 nm) and in a dark-adapted form ($bR^{DA}_{558}$; $\lambda_{max}$ 558 nm). The chromophore of the light--adapted form is an all-*trans* retinylidene moiety, bound as a protonated *Schiff* base to Lys 216[2,3]. In the dark-adapted form ($bR^{DA}$), a 3/2 equilibrium exists between 13-*cis* ($bR_{548}$) and all-*trans* ($bR_{568}$) isomers[2,3].

Model protonated *Schiff* bases of all-*trans* retinal (**1**) and *n*-butylamine in methanol absorb around 440 nm. It is clear that the interaction of the chromophore with the peptide chain in $bR_{568}$ and $bR_{548}$ causes the shift from 440 nm to 568 nm and 548 nm, resp. This difference in $\lambda_{max}$ value of the protein, compared with the free chromophore, is called opsin shift (expressed in $cm^{-1}$)[4].

$^{13}C$ NMR experiments[5] have shown that in $bR_{548}$ and $bR_{568}$ the chromophores occur in planar C6–C7 *s*-*trans* conformation and that the positive charge on C5 is higher than in model protonated *Schiff* bases, due to a negative charge in